Spatial-Angular Selectivity of 3-D Speckle-Wave Holograms and Information Storage

Vladimir B. Markov*

Institute of Applied Optics, The National Academy of Sciences of Ukraine, 10-G Kudrjavskaja St., Kyiv, 254053, Ukraine

The properties of volume holograms recorded with speckle reference wave are of interest because they allow high-density information multiplexing and its coding and processing. The results of theoretical and experimental study of angular selectivity for this type of hologram are presented in this article. Several mechanisms are interacting in this case as a result of the joint action of cross modulation grating (diffraction on cross grating) and intermodulation structure (locally recorded speckle pattern). The conditions are determined when the value of the angular selectivity depends either on the cross grating spacing or on the speckle pattern parameters. The strong angular selectivity of the speckle-wave hologram can be observed by its angular detuning in any arbitrary direction. It is demonstrated that observed peculiarities in the character of angular selectivity of the hologram with reference speckle wave can be very efficient for multiple holographic image recording in thick media.

Journal of Imaging Science and Technology 41: 383–388 (1997)

Introduction

Volume phase holograms, in particular those recorded with spatially nonuniform waves, are of interest because they can be used for high-density memory systems,[1–3] neural networks[4] and high-precision shift measurements.[5] The spectral and angular selectivity of volume holographic gratings in combination with the conservation momentum law,[6] allow the realization of these applications. However, the expressions derived in Ref. 7 for dispersion of volume sinusoidal gratings cannot be used to describe selective characteristics of gratings with more complicated structures.

Theoretical analysis of volume holograms recorded by spatially nonuniform waves were made by several authors.[8–12] It was demonstrated experimentally[13] that maximal intensity of the diffracted signal can be reached at hologram angular deviation from its exact Bragg position within its angular selectivity $\delta\theta_H$. The dispersion characteristics of the hologram recorded with speckle reference wave, as shown in Refs. 14 and 15, exhibit some deviation from the rules typical for the plane-wave volume hologram.

In this article, the angular selectivity of volume holograms recorded with the reference speckle wave is studied. The possibility of using this type of selectivity for multiple-image recording is also demonstrated.

Theoretical Analysis

Model of the Reference Speckle Wave Hologram. Let us consider a volume phase hologram recorded with reference speckle wave $\vec{R}_0(\vec{r})$ of the divergence θ_{SP} and plane wave $\vec{S}_0(\vec{r}) = a \cdot \exp(i\vec{k}_{S0}\vec{r})$ of the amplitude a (Fig. 1). Here $\vec{r} = f(\vec{q}, z)$ is the spatial vector with its transversal component $\vec{q}$ in the hologram plane; $\vec{k}_{S0} = \vec{k}_0$ ($\sin\theta_{S0}$, $\cos\theta_{S0}$) is the wave vector in the direction of plane wave propagation; and

$$\left|\vec{k}_0\right| = 2\pi/\lambda,$$

λ is the wavelength. The central direction of propagation for the wave $\vec{R}_0(\vec{r})$ is selected to be normal to the hologram front surface. Then, θ_{S0} is an angle between two interacting waves ($\theta_{S0} >> \theta_{SP}$).

The amplitude function[16] of the speckle wave $R(\vec{r})$ formed after the diffuser Φ with random transmission function

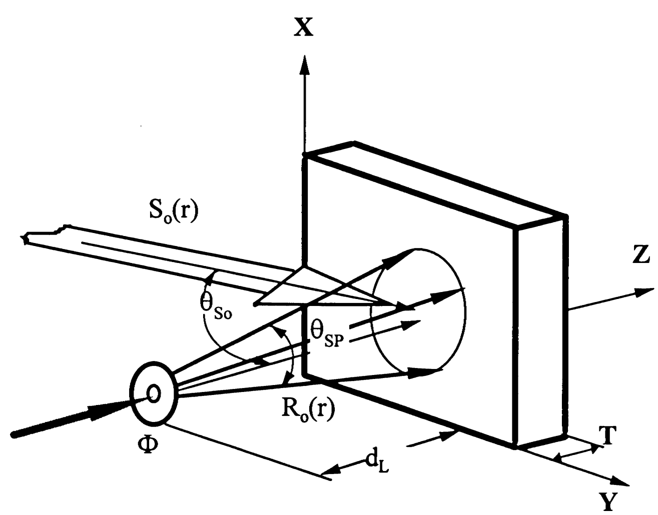

Figure 1. Geometry of the 3-D hologram recording by signal plane wave $\vec{S}_0(\vec{r})$ and reference speckle wave $\vec{R}_0(\vec{r})$ of the angular divergence θ_{SP}. Here T is recording media thickness, θ_{S0} is an angle between recording beams; Φ_D is the diameter of the illuminated part of the diffuser Φ, and D_H is the diameter of the hologram.

Original manuscript received February 7, 1997.

* Present address: Centro International de Fisica, A.A. 4948 Bogotá, Colombia

©1997, IS&T—The Society for Imaging Science and Technology

$$t(\vec{q}_1) = t_0 \sum_{m=0}^{N} \exp(i_{\alpha_m}) \delta(\vec{q}_1 - \vec{q}_m)$$

can be written as[17]

$$R(\vec{q}, z) \cong t_0 \sum_{m=0}^{N} \exp(i_{\alpha_m}) \exp\left[\frac{-i_{k_0}}{2d_L}(\vec{q}_1 - \vec{q}_m)\right], \qquad (1)$$

where $\delta(\vec{q}_1 - \vec{q}_m)$ is Dirac's delta function, α_m is the phase coefficient, and $\vec{q}_1 = (x_1, y_1)$. It is assumed in Eq. 1 that the distance diffuser-hologram (or lens-hologram) is much higher than the recording media thickness, i.e., $d_L >> T/n$.

We assume that after exposure the permifflvity $\varepsilon(\vec{r})$ of the recording material will exhibit local changes $\varepsilon(\vec{r}) = \varepsilon_0 + \delta\varepsilon(\vec{r})$ and $\delta\varepsilon(\vec{r})$ is the modulated component of the permittivity. The value of $\delta\varepsilon(\vec{r})$ is supposed to be proportional to the square of the electric field of the interacting waves, i.e.,

$$\delta\varepsilon(\vec{r}) \sim |E|^2 = \left|\vec{S}_0(\vec{r}) + \vec{R}_0(\vec{r})\right|^2.$$

Let us consider reconstruction of the hologram on a small angle $\delta\theta_A << \theta_{S0}$ of deviation with respect to the recording position. The same speckle wave $\vec{R}_0(\vec{r})$ is used at the reconstruction step, illuminating the hologram at new angle of incidence $\theta_S = \theta_{S0} + \delta\theta_A$. Propagation of transmitted $\vec{R}(\vec{r})$ and diffracted $\vec{S}(\vec{r})$ waves in the volume of the hologram can be described through the system of Maxwell's equations.[11] For the monochromatic waves of identical polarization in an isotropic media, the system can be reduced to a scalar wave equation

$$\Delta E(\vec{r}) + \left[\varepsilon_0 + \delta\varepsilon(\vec{r})\right] k_0^2 E(\vec{r}) = 0 \qquad (2)$$

and the condition $\Delta \mathrm{div} E(\vec{r}) = 0$ serves as the validity criterion for Eq. 1.

Diffracted Field Calculation. To solve Eq. 2 the following assumptions were made:

(1) Bragg type of diffraction is assumed, which imposes some limitations on the values of θ_{S0}, θ_{SP}, and medium thickness T. These limitations can be expressed[9] as $T \geq \lambda/(\Delta\theta_{SP})^2 \geq \lambda/\theta_{S0}$;

(2) the magnitude of the wave $R(\vec{r})$ is much greater than the diffracted signal $S(\vec{r})$—*the undeplation field (UDF) approximation.*

Assumption (2) allows us to apply the perturbation theory method[18] to solve Eq. 2. In this case the field E is sought as a power series of $\delta\varepsilon(\vec{r})$. Then differential Eq. 2 can be transformed to an integral one and its solution now will be sought as

$$E(\vec{r}) = R(\vec{r}) + \sum_{m=1}^{\infty} S_m(\vec{r}), \qquad (3)$$

where $S_m(\vec{r})$ are the terms of the Neumann series. However, taking into account assumption (1), the summation

$$\sum_{m=1}^{\infty} S_m(\vec{r})$$

in Eq. 3 can be limited to the first term—first Born approximation. Also replacing $\delta\varepsilon(\vec{r})$ in Eq. 2 by the term $R(\vec{r}) \cdot R^*(\vec{r})$, which is responsible for $R(\vec{r}) \Rightarrow S(\vec{r})$ transformation, the diffracted wave can be presented as

$$S(\vec{r}) \cong -k_0^2 \int_{-\infty}^{+\infty} P_V(\vec{r}\,') R_0^*(\vec{r}) R(\vec{r}\,') G(\vec{r}, \vec{r}\,') \exp(i_{k_s} \vec{r}\,') d^3 r'; \qquad (4)$$

here

$$G(\vec{r}, \vec{r}\,') = -\frac{1}{4\pi} \frac{\exp\left[ik_0 |\vec{r}, \vec{r}\,'|\right]}{|\vec{r}, \vec{r}\,'|}$$

is Green's function.

Diffracted Signal at Hologram Angular Deviation. Evident now from Eq. 4 is that any transformations in the structure of the reconstructing wave, compared to the recording one $R(\vec{r})$ will lead to changes of the diffracted wave amplitude $S(\vec{r})$. The sensitivity of the diffracted signal with respect to the hologram angular deviation from the Bragg conditions is now considered. This operation is equivalent to the synchronous rotation and shift of the speckle wave, and the OY axis is selected for rotation in this analysis.

Because the reconstructing speckle wave $R_0(\vec{r})$ illuminates the hologram at an angle which deviates by a small value $\delta\theta_A$ ($\delta\theta_A << 1$) from its initial recording position, its amplitude can be described by an equation similar to Eq. 1 but with new coordinates $\vec{r}\,' = (\vec{q}\,', z')$. Thus, the amplitude of the reconstructing wave $R(\vec{r})$ can be expressed as[16]

$$R(\vec{q}, z') = t_0 \sum_{m=0}^{N} \exp(i\alpha_m) \exp \left\{\frac{-ik}{2d_L^0}\left[(x' - z'\,\delta\theta_A - x_m)^2 + (y' - y_m)^2\right]\right\}. \qquad (5)$$

Substituting Eq. 5 in Eq. 4, the diffracted wave amplitude can be written in the form

$$S(\delta\theta_A \vec{q}\,') = \exp(\vec{k}_0 \sin\theta_S) t_0^2 \int_0^T \frac{1}{z'\,\delta\theta_A} \exp \left\{\frac{-ik_0 \delta\theta_A}{d_L}(z'\,\delta\theta_A + 2y)\right\} J_1\left(\frac{k_0 \Phi_L \delta\theta_A}{2d_L}\right) dz', \qquad (6)$$

where $J_1(p)$ is the first-order Bessel function of the first kind and Φ_L is the diameter of the illuminated part of the diffuser Φ.

Finally, from. Eq. 6, the expression for the diffracted wave intensity $I_D(\delta\theta_A)$ can be derived. However, to compare with the experimental data it is more convenient to use the normalized value of the diffracted beam intensity $I_D(\delta\theta_A)/I_{D\max}$, where $I_{D\max} = I_D(\delta\theta_A = 0)$ is the diffracted signal value at the exact Bragg conditions. Then Eq. 6 can be used in the following form

$$\frac{I_D(\delta\theta_A)}{I_{D\max}} = \frac{1}{\pi}\left(\frac{4d_L}{k_0 D_H \Phi_L T}\right) \iint_{0 \leq q^2 \leq D_H^2/4} \left|S(\delta\theta_A, \vec{q}\,')\right|^2 d^2 q'. \qquad (7)$$

Expression 7 describes the dependence of the diffracted beam intensity normalized to its maximum value on angular deviation of the hologram relative to the reconstructing speckle wave. This can be also considered as the function of diffraction efficiency $\eta(\delta\theta_A)$ of the hologram reconstructed with speckle wave.

Analysis of the Hologram Angular Deviation. Following the theoretical analysis, we will consider now the

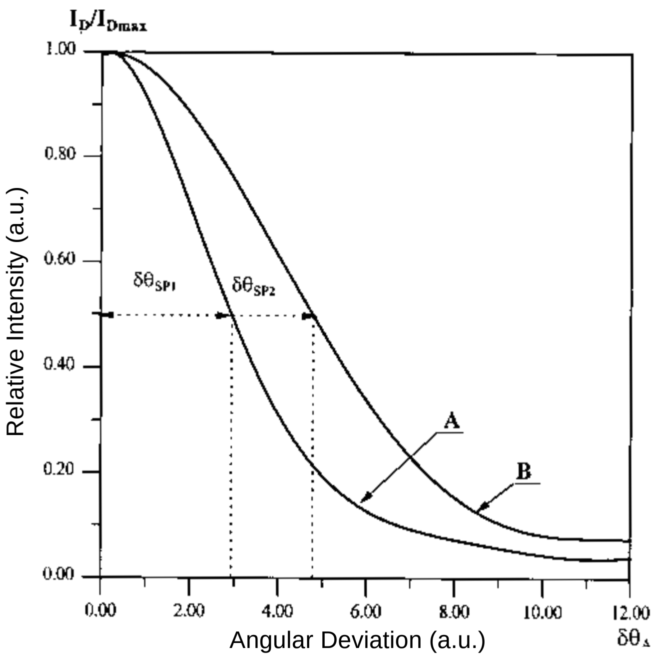

Figure 2. Calculated dependence of the normalized diffracted bearn intensity $I_D/I_{D\max}$ on hologram angular deviation $\delta\theta_A$ at reconstruction with reference speckle wave with different average speckle sizes: A— $\sigma_\perp$ = 8.0 μm; B— $\sigma_\perp$ = 16.0 μm (T = 2 mm, λ = 441.6 nm).

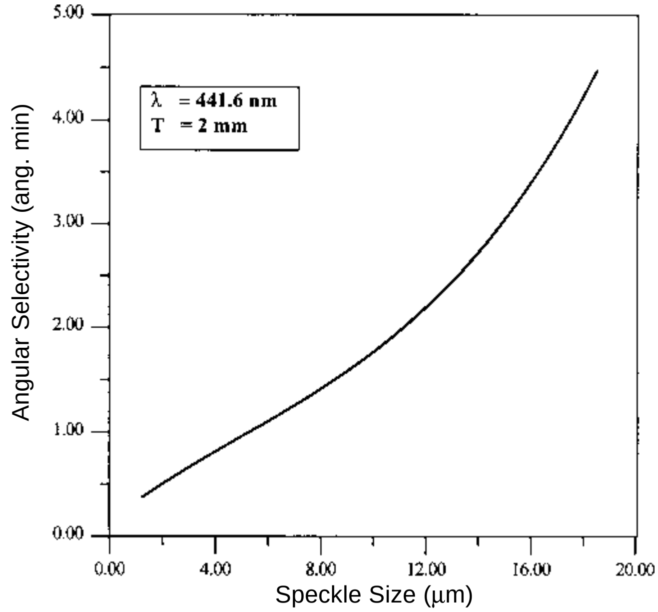

Figure 3. Calculated dependence of angular selectivity $\delta\theta_{SP}(\sigma_\perp)$.

sensitivity of the diffracted signal $I_D(\delta\theta_A)$ to angular deviation of the hologram around the OY axis. Usually, tilt of the hologram in this direction has a very small effect on the diffracted signal value.[7] Figure 2 plots the dependence $I_D/I_{Dmsx}(\delta\theta_A)$ obtainable from Eq. 7. The values of the recording wavelength λ, crystal thickness T, and speckle wave parameters (θ_{SP} and d_L) selected to simulate this dependence are identical to those of experiments. The calculated function $I_D/I_{D\max}(\delta\theta_A)$ has a monotonic character and smoothly falls with increase of $\delta\theta_A$. Unlike angular selectivity of the conventional plane-wave volume holographic grating, no oscillations of $I_D/I_{D\max}(\delta\theta_A)$ function occur in this case.

Obviously, when $\theta_S \neq \theta_{S0}$, the individual speckles in the reconstructing pattern, are not synchronized any more with the speckle cells recorded in the the hologram. Their spatial/angular mismatch increases with increase of $\delta\theta_A$. Diffracted signal intensity $I_D(\delta\theta_A)$ should therefore depend on such parameters as lateral $\sigma_\perp \sim 1.22\lambda / \theta_{SP}$ and longitudinal $\sigma_\| \sim 8\lambda / (\theta_{SP})^2$ correlation radii of the speckle structure, known as average speckle size.[16] So Fig. 2 serves to compare the angular response of the reconstructed beam intensity upon the variations of the last one.

For volume grating angular selectivity, $\delta\theta_{GR} \approx \lambda/2T\sin\theta_S$ is the parameter used to characterize dependence of the diffracted beam intensity upon hologram angular deviation from the exact Bragg conditions. By analogy, the speckle selectivity $\delta\theta_{SP}$ can be introduced here, which corresponds to angular deviation $\delta\theta_A$ such that $I_D/I_{D\max} = 0.5$. The actual value of $\delta\theta_{SP}$ for the fixed hologram thickness T can be connected with the average speckle size $\sigma_\perp$ in the recording reference wave. We have to admit that the effects of the Bragg selectivity are usually very small at hologram angular deviation in the direction perpendicular to the dispersion plane (around the OY axis) and, therefore, influence of the cross-grating selectivity should be negligibly low here. However, presence of the speckle structure in one of recording beam changes the properties of the hologram, and selectivity is one of the detectable results of these changes. Variation of the speckle size $\sigma_\perp$ affects the final value of $\delta\theta_{SP}$. In particular, increase of $\sigma_\perp$ leads to corresponding broadening of the magnitude of $\delta\theta_{SP}$, demonstrated in Fig. 3. Here the half-width of the angular selectivity $\delta\theta_{SP}$ is plotted as the function of the average speckle lateral size $\sigma_\perp$ at hologram rotation around the OY axis.

The recorded speckle wave hologram is an ensemble of individual speckles modulated by the cross grating. The process of diffraction when the speckle wave is used for reconstruction may be considered as self-correlated interaction between recorded and reconstructing structures. Then, the principal mechanism of the angular selectivity in the above case can be connected with spatial/angular decorrelation of the speckle structure recorded in the volume of the hologram and that used to reconstruct the hologram at new angle θ_S. This angular mismatch, as follows from Eq. 6, should affect both the amplitude and phase of the partial waves diffracted on the individual speckles. Decrease in the amplitude of these partial waves may be connected with spatial decorrelation of the recorded and read out structures. That is what differentiates volume speckle-wave holograms from traditional volume diffraction gratings, where dephasing factors of the reconstructing and diffracting waves play the same role.

Experimental Part

Experimental Technique. A standard two-beam setup was used in the experiments performed to record the phase volume hologram with reference speckle wave. A phase diffuser introduced in one of the recording beams was used to form the speckle pattern in the plane of the light-sensitive media. The second arm of the optical setup had a telescope and diaphragm to form a low-divergence beam (plane wave) with its cross section equal to the speckle beam in the recording plane (D_H = 8 mm). The cross-grating spacing was in the range Λ ~ 5 to 0.9 μm (θ_{S0} = 5° ± 30°).

A He-Cd laser (λ = 441.6 nm, P ~ 50 mW) was used as a coherent light source to record volume phase holograms in

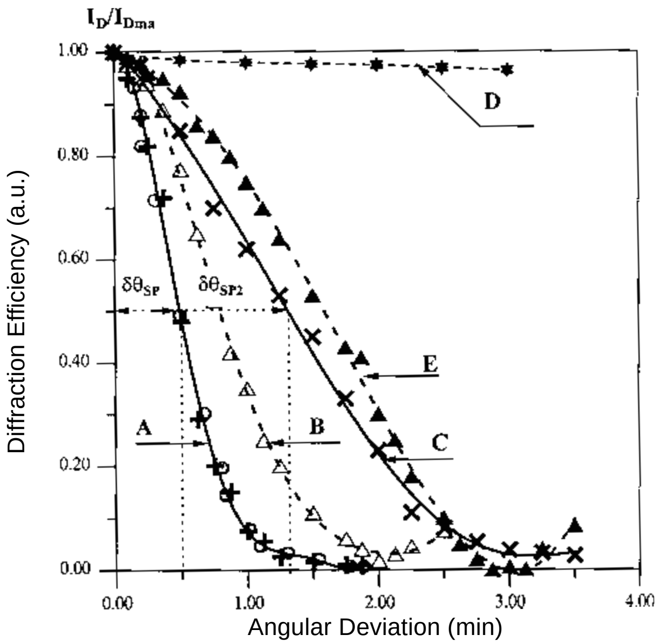

Figure 4. Experimental dependence of the relative diffracted beam intensity $I_D/I_{D\max}$ on hologram angular deviation $\delta\theta_A$: Tilt of the hologram in the direction perpendicular to dispersion plane (around the OY axis). Speckle wave hologram: A[+] — $\sigma_\perp \approx 2.0$ μm, $\Lambda = 1.2$ μm; C— $\sigma_\perp \approx 6.0$ μm; $\Lambda = 1.2$ μm. Plane wave hologram: D—$\Lambda = 1.2$ μm. Tilt of the hologram in the dispersion plane (around the OX axis): Speckle wave hologram: A[0]— $\sigma_\perp \approx 2.0$ μm, $\Lambda = 1.2$ μm, E— $\sigma_\perp \approx 10.0$ μm, $\Lambda = 2.0$ μm, Plane wave hologram: B—$\Lambda = 1.2$ μm.

T = 2-mm-thick crystal $LiNbO_3$: Fe (0.03 mass %). The C axis coincides with the plane of polarization of the recording beams. According to the theoretical analysis, the crystal's front surface was set perpendicular to the central direction of the speckle wave propagation. A piezoelectric actuator was used to tilt the hologram with the accuracy of $\pm 0.3 \times 10^{-4}$ rad.

Maximum diffraction efficiency of the recorded hologram did not exceed 10% to tolerate the UDF approximation. To avoid the effect of energy transfer, related to bending of the holographic fringes,[19] the average intensity of both recording beams was adjusted to be equal. The speckle beam of attenuated intensity was used to reconstruct the diffracted signal.

Experimental Results and Discussions. As follows from the **Theoretical Analysis**, the intensity of the diffracted signal at hologram angular deviation is substantially affected by the average speckle size $\sigma_\perp$. Figure 4 illustrates typical experimental dependencies of the relative diffracted beam intensity $I_D(\delta\theta_A)/I_{D\max}$ for several values of $\sigma_\perp$. Here, Curves A [+] and C correspond to the speckle wave hologram ($\sigma_\perp \approx 2$ and 6 μm respectively, Λ = 1.2 μm) tilted around the OY axis. Obviously, increase of $\sigma_\perp$ increases the corresponding value of $\delta\theta_{SP}$. It is known[7] that the plane wave hologram has very low selectivity with regard to its rotation in direction normal to the dispersion plane (around the OY axis). This is illustrated by Curve D, measured for the grating with Λ = 1.2 μm. At the same time, presence of the speckle structure the in reference beam significantly changes the properties of the selectivity (Curve A[+]). In particular, speckle structure makes it possible to increase selectivity in this direction.

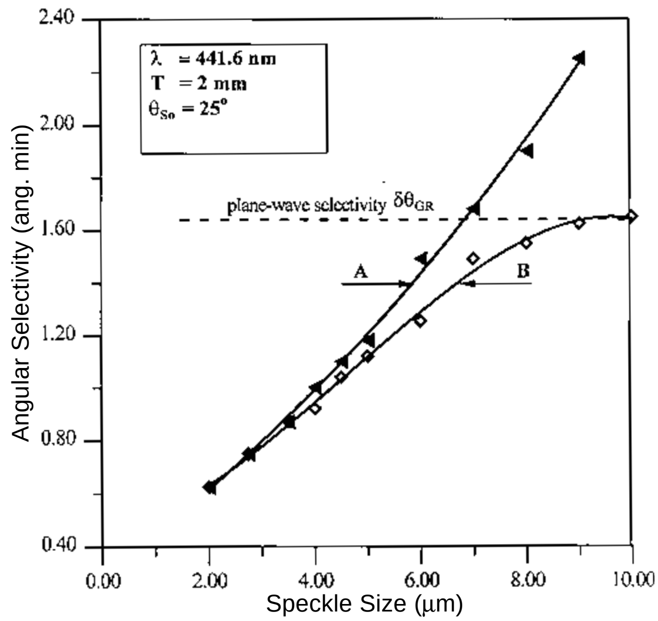

Figure 5. Angular selectivity $\delta\theta_H$ as a function of the average speckle sizes $\sigma_\perp$ for hologram angular deviation around OY (A) and OX (B) axis. Dashed line corresponds to angular selectivity of the pure cross grating $\delta\theta_{GR}$ recorded by plane waves in identical conditions.

The magnitude of the selectivity with regard to hologram rotation in its dispersion plane depends on recording conditions. For instance, it follows from comparison of Curves A[0] and B recorded with identical Λ = 1.2 μm, that for certain experimental situations, the value of $\delta\theta_{SP}$ can be less than the corresponding selectivity $\delta\theta_{GR}$ of the cross grating. However, increase of $\sigma_\perp$ leads to the broadening of $\delta\theta_{SP}$, and as a result conditions can be reached where angular selectivity of the speckle wave hologram is determined mainly by traditional parameters of the cross grating (Curve E: Λ = 2 μm; $\sigma_\perp \approx 10$ μm).

The dependence of $\delta\theta_{SP}(\sigma_\perp)$ derived from $I_D(\delta\theta_A)$ is presented in Fig. 5 (Curve A). When the hologram is tilted around the OY axis, the value of $\delta\theta_{SP}$ monotonically increases with increase of $\sigma_\perp$ which corresponds to theoretical analysis (Fig. 3). Because the angular selectivity of the cross grating ($\delta\theta_{GR}$) at such rotation is exceedingly low, the character of the selectivity is determined mainly by spatial decorrelation between recorded and retrieving speckle structures.

The character of angular selectivity with regard to hologram angular deviation in the plane of dispersion (around the OX axis) has more complicated behavior because it is governed by a joint action of two mechanisms: regular angular selectivity of the cross grating, and the discussed speckle selectivity. It is more convenient to introduce general selectivity of the hologram $\delta\theta_H$ in this case. As seen from Fig. 5 (Curve B), the interaction between two factors determines the actual behavior of the dependence $\delta\theta_H(\sigma_\perp)$ here. When the dimensions of the speckles $\sigma_\perp$ are comparable with the grating spacing Λ, speckle selectivity strongly dominates over cross grating one, i.e., $\delta\theta_{SP} << \delta\theta_{GR}$. For the discussed experimental results, this fits the conditions when $\sigma_\perp < 5$ μm. With further increase of $\sigma_\perp$, the speckle selectivity $\delta\theta_{SP}$ plays a progressively less essential role, while cross grating selectivity becomes a dominating mechanism and determines the actual angular selectivity $\delta\theta_H$ (for $\sigma_\perp > 6$ μm). Finally, for $\sigma_\perp > 9$

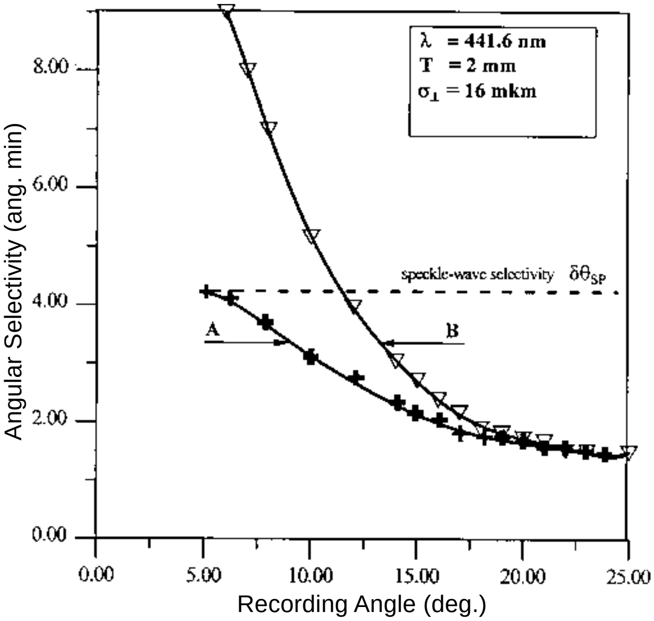

Figure 6. Angular selectivity $\delta\theta_H$ as a function of recording angle θ_{S0} at hologram angular deviation around OX axis for plane wave (A) and speckle wave (B) holograms. Dashed line corresponds to angular selectivity of speckle wave hologram $\delta\theta_{SP}$ at its tilt around OY axis.

μm, $\delta\theta_H$ reaches its maximal value ($\delta\theta_H$ = 1.65 ang. min), which is limited by the angular selectivity of the cross grating $\delta\theta_{GR}$ (dashed line) and remains unchanged with further increase of $\sigma_\perp$.

Similar transition from speckle to cross grating selectivity can be attained by changing the recording angle θ_{S0} while leaving fixed the value of $\sigma_\perp$. The cross grating selectivity $\delta\theta_{GR}$ is known to become sharper with the increase of θ_{S0} (decrease of Λ). This is illustrated by Fig. 6 (Curve B), where experimental dependence $\delta\theta_{GR}(\theta_{S0})$ for the standard plane-wave hologram is presented. As in a previous case, the character of speckle wave hologram selectivity $\delta\theta_H$ is governed by the joint action of cross grating and speckle structure (Fig. 6, Curve A). Here, the contour $\delta\theta_H$ is shown for the hologram with $\sigma_\perp \approx 16$ μm. So for the recording angle $\theta_{S0} < 12°$ ($\Lambda > 2.3$ μm), the major influence on the value of selectivity is speckle decorrelation. Increase of θ_{S0} is followed by the corresponding growth of the influence of the cross-grating on the measured magnitude of $\delta\theta_H$ and in the range $12° < \theta_{S0} < 16°$ ($1.6 < \Lambda < 2.3$ μm). The actual value of $\delta\theta_H$ is determined by both mechanisms. Finally, at large enough recording angles, $16° < \theta_{S0}$ ($\Lambda <$ 1.6 μm), the character of the angular selectivity is totally controlled by the cross grating. However, acting on the level of the speckle wave selectivity (dashed line) through alteration of the value of $\sigma_\perp$, it is possible to control the actual level of angular selectivity $\delta\theta_H$ of the hologram.

As indicated in **Analysis of the Hologram Angular Deviation** above, the decline in the spatial by overlapping area of the recorded/reconstructing speckles owing to their spatial mismatch at hologram angular deviation may be considered as one of the reasons responsible for the decrease of the diffracted signal amplitude. Let us estimate the magnitude of this spatial mismatch. Obviously, the maximal value of the shift will be observed for the speckles located at the hologram periphery. The maximum lateral $\Delta_\perp$ and longitudinal $\Delta_\parallel$ shift of the individual speckle will amount, respectively, to

$$\Delta_\perp \cong \frac{T\delta\theta_A}{n} + \frac{D_H^2\delta\theta_A}{4nd_L}, \quad \Delta_\parallel \cong \frac{D_H\delta\theta_A}{2}, \tag{8}$$

where $n \approx 2.24$ is the refraction index of $LiNbO_3$ crystals.

Now, to calculate the conceivable magnitudes of lateral and longitudinal speckle decorrelation we will select the experimental data that correspond to the largest angular deviation ($\delta\theta_{SP}$ = 4.5 ang. min. at d_L = 80 mm, T = 2 mm, and D_H = 8 mm). In this case, as follows from Eq. 8, the calculated magnitude of the individual speckle mismatch owing to angular deviation of the hologram can reach $\Delta_\perp$ = 1.2 μm and $\Delta_\parallel$ = 4.8 μm, respectively. However, as shown in Refs. 5 and 15, the diffracted beam intensity decreases practically to zero when the lateral or longitudinal shift of the hologram ranges up to the distance equal to the average lateral or longitudinal speckle size. For the experimental conditions under consideration, this should be $\sigma_\perp \cong 15$ μm and $\sigma_\parallel = 2.5$ μm, respectively, i.e., the values which far exceed the magnitudes of the speckle shift calculated from Eq. 8. Following these results, the assumption can be made that spatial decorrelation of the recorded/ reconstructing speckle structures leads to destructive interference of the partial components of the diffracted wave. Similar to the diffraction on plane-wave volume gratings, this results in reduction of the diffracted beam intensity for hologram angular deviation from the exact Bragg position.

Holographic Image Multiplexing with Angular Speckle Selectivity

Volume holographic memory seems an efficient way for high-density 3D information storage.[1,2] The holograms are usually recorded through angular,[20–22] wavelength,[3,23] or phase-coded multiplexing.[24] The possibility of spatial multiplexing by use of the speckle wave or M-number plane-wave reference beam[26] was also demonstrated. The discussed effects of speckle angular selectivity also can be used for information storage and image multiplexing in volume holograms. Two advantages over the other known methods are indicated here: First, the reference speckle wave allows increase of the number of multiplexed records owing to arbitrary direction of the hologram angular deviation, not only in its dispersion plane. This is of importance, for instance, for ferroelectric crystals like $LiNbO_3$ with strong dependence of the recording efficiency on holographic fringe orientation. Then, the speckle wave recording demonstrates decrease of oscillations of diffracted signal intensity at holograms out of Bragg reconstruction, typical for plane-wave hologram that can be used to reduce the level of cross talk.

Figure 7 illustrates an example with reconstruction of four images using the features of 3D speckle-wave hologram selectivity. The actual images have been stored in 2-mm-thick Fe:$LiNbO_3$ without its spatial shifting.[25] For this experiment the recording geometry of Fig. 1 was modified and the transparency was placed in the arm of signal beam S. The image of this transparency was formed behind the crystal by the positive lens and then photographed. This image signal beam (defocused in the plane of the recording media) interfered with the speckle reference wave in the volume of the crystal.

Four images (2 × 2 matrix) have been recorded sequentially using angular multiplexing in two orthogonal directions. The hologram recording on the central peak of the angular selectivity, which is common for both directions of the angular deviation, was omitted to avoid the

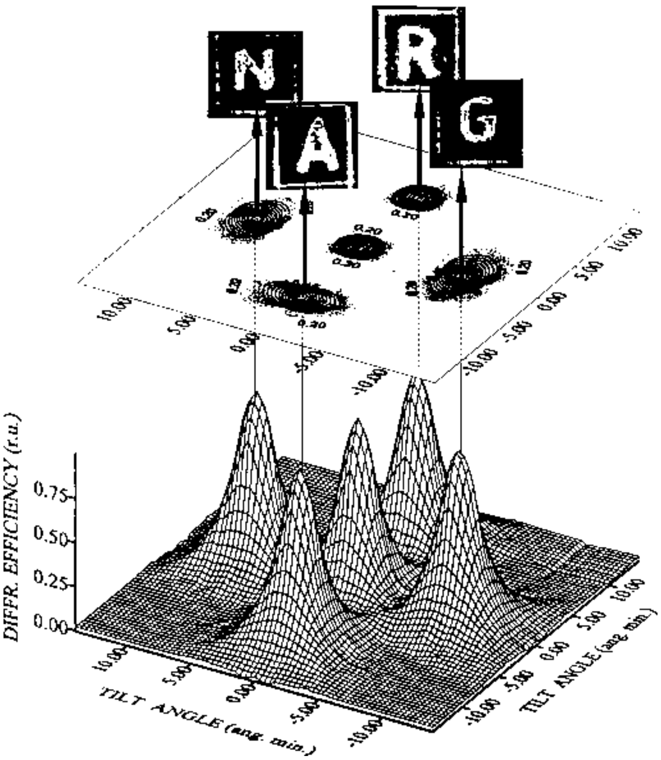

Figure 7. Reconstruction of angular-multiplexed images stored in 2-mm-thick $Fe:LiNbO_3$ crystal. The multiplexing was made by hologram angular deviation in the plane of dispersion (images N and G) and in orthogonal direction (images A and R).

overlapping (degeneration) of the reconstructed images. For multiple recording, two images first were stored through the angular tilt of the crystal within the dispersion plane of the hologram. The recording conditions were identical to those of Fig. 4, where speckle selectivity exceeds the cross grating one. Then, the other two images were recorded in the perpendicular direction. These four recorded images were easy to reconstruct through the corresponding angular positioning of the crystal illuminated with the reference speckle wave (Fig. 7).

Conclusions

In this article the peculiarities of the angular selectivity of volume holograms recorded with the speckle reference wave were studied. In contrast to the angular selectivity of the conventional plane-wave volume hologram connected by the phase mismatch of the diffracted and reconstructing waves on the recorded cross grating, the results obtained illustrate a new kind of angular selectivity. The mechanism of this selectivity is due to amplitude phase mismatch between the speckle structures of the recorded and reconstructing waves. The width of this speckle angular selectivity depends on the value of the average speckle size in the reference wave in the plane of the hologram.

Because the recorded speckle pattern is statistically uniform in any direction perpendicular to its propagation wave vector, the speckle angular selectivity turns out to be independent of the choice of the axis of the hologram angular deviation. The character of angular selectivity for hologram deviation in the dispersion plane is governed by the joint action of the recorded cross grating and speckle structure.

We demonstrated that the features of angular selectivity of the holograms recorded with the speckle reference wave allows image multiplexing within angular selectivity of standard cross gratings and in the direction perpendicular to the dispersion plane of the hologram, where normally very low angular selectivity is observed. ▲

Acknowledgments. This work was supported by the Colombian Institute for the Development of Sciences and Technology (COLCIENCIAS) through Grant No. 2228-05-401-93. The author is also grateful to International Institute of Theoretical Physics (ICTP) for Grant VS-186 and to Dr. A. Darskiy for fruitful discussions.

References

1. P. J. van Heerden, Theory of optical information storage in solids, *Appl. Opt.* **2,** 393–400 (1963).
2. L. K. Anderson, Holographic optical memory for bulk data storage, *Bell Lab. Rec.* **46,** 318–324 (1968).
3. G. A. Raculich, V. Leyva, and A. Yariv, Optical data storage by using orthogonal wavelength-multiplexed/demultiplexing of volume hologram in photorefractive media, *Opt. Lett.* **18,** 534–536 (1993).
4. K. Wagner and D. Psaltis, Multilayer optical learning networks, *Appl. Opt.* **26,** 5061–5076 (1987).
5. A. Darskii and V. Markov, Measurements of small displacements by speckle holography, *Opt. Las. Technol.* **21,** 198–203 (1989).
6. W. L. Bragg, The diffraction of the short electromagnetic waves by crystal, *Proc. Camb. Phil. Soc.* **17,** 43–57 (1912).
7. H. Kogelnik, Coupled wave theory for thick holographic gratings, *Bell Syst. Technol. J.* **48,** 2909–2947 (1969).
8. Yu. Denisyuk, About the reproduction of the optical properties of the object in the wave field of scattered emission, *Dokl. Akad. Nauk SSSR,* **144,** 1275–1278, 1962.
9. V. G. Sidorovich, Theory of the light waves transformation by 3D hologram, *Opt. Spectrosc.* **44,** 302–305 (1978).
10. B. Ya. Zeldovich, V. V. Shkunov, and T. V. Yakovleva, Speckle fields holograms, *Usp. Phys. Nauk* **149,** 511–549 (1986).
11. L. Solimar and D. J. Cooke, *Volume Holography and Volume Gratings, Academic Press,* 1981.
12. Yu. Korzinin and V. Sukhanov, Diffraction efficiency of the 3D phase hologram of the diffuse object, *Opt. Spectrosc.* **58,** 142–146 (1985).
13. E. A. Sander, V. V. Shkunov, and C. A. Shoidin, Experimental observation of the spatial resonance of the speckle field with the non-uniformity of the reflection index, *J. Theor. Exper. Phys.* **88,** 116–119 (1985).
14. V. B. Markov, V. F. Shishkov, and A. I. Khiznijak, Angular selectivity of the volume holograms recorded by speckle structure, *Ukr. Fiz. Zh.* **30,** 508–510 (1985).
15. A. M. Darsky, and V. B. Markov, Shift selectivity of the holograms with the reference speckle wave, *Opt. Spectrosc.* **65,** 661–665 (1988).
16. G. W. Goodman, Statistical properties of laser speckle patterns, in *Laser Speckle and Related Phenomena,* J. C. Dainty, Ed. (Springer-Verlag, Berlin, 1975).
17. J. C. Dainty, The Statistics of Speckle Pattern, E. Wolf, Ed., in *Progress in Oprics XIY,* North Holland, 1976.
18. V. I. Tatarski, *Wave propagation in a Turbulent Medium,* McGraw-Hill, New York, 1961.
19. N. Kukhtarev, V. Markov, and S. Odulov, Transient energy transfer during hologram formation in $LiNbO_3$ in external electric field, *Opt. Commun.* **23,** 338–343 (1977).
20. L. d'Auria, J. P. Huignard, C. Slezak, and E. Spitz, Experimental holographic read–write memory, using 3-D *storage, Appl. Opt.* **13**, 808–818 (1974).
21. S. Tao, D. Selviah, and J. Midwinter, Spatioangular multiplexed storage of 750 holograms in an $Fe:LiNbO_3$ crystal, *Opt. Lett.* **18,** 912–914 (1993).
22. F. Mok, Angular-multiplexed storage of 5000 holograms in lithium niobate, *Opt. Lett.* **18,** 915–917 (1993).
23. J. Rosen, Wavelength-multiplexed computer-generated volume holography, *Opt. Lett.* **18,** 744–746 (1993).
24. T. F. Krile, R J. Marks, J. F. Walkup, and M. O. Hagler, Multiplexed Holographic representations of space-invariant system using phase-coded reference beams, *Appl. Opt.* **16**, 3131–3135 (1977).
25. V. Markov, Display and applied holography for culture development, *Proc. SPIE* **IS-8,** 268–304 (1990).
26. D. Psaltis, M. Leven, A. Pu, G. Barbastathis, and K. Kurtis, Holographic storage using shift multiplexing, *Opt. Lett.* **20,** 782–784 (1995).